

Mechanism of α -Amino Acids Decomposition in the Gas Phase. Experimental and Theoretical Study of the Elimination Kinetics of N-Benzyl Glycine Ethyl Ester

Maria Tosta,[†] Jhenny C. Oliveros,[‡] Jose R. Mora,[†] Tania Córdova,[‡] and Gabriel Chuchani^{*†}

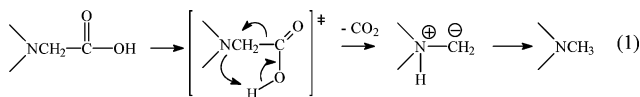
Centro de Química, Instituto Venezolano de Investigaciones Científicas (I.V.I.C.), Apartado 21827, Caracas, Venezuela and Escuela de Química, Facultad de Ciencias, Universidad Central de Venezuela, Apartado 1020- A, Caracas, Venezuela

Received: November 16, 2009; Revised Manuscript Received: January 20, 2010

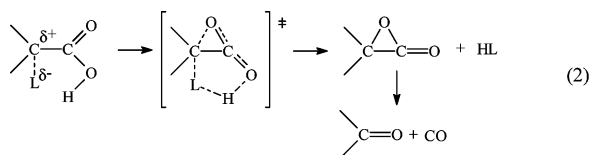
The gas-phase elimination kinetics of N-benzylglycine ethyl ester was examined in a static system, seasoned with allyl bromide, and in the presence of the free chain radical suppressor toluene. The working temperature and pressure range were 386.4–426.7 °C and 16.7–40.0 torr, respectively. The reaction showed to be homogeneous, unimolecular, and obeys a first-order rate law. The elimination products are benzylglycine and ethylene. However, the intermediate benzylglycine is unstable under the reaction conditions decomposing into benzyl methylamine and CO₂ gas. The variation of the rate coefficients with temperature is expressed by the following Arrhenius equation: $\log k_1 \text{ (s}^{-1}\text{)} = (11.83 \pm 0.52) - (190.3 \pm 6.9) \text{ kJ mol}^{-1} (2.303RT)^{-1}$. The theoretical calculation of the kinetic parameters and mechanism of elimination of this ester were performed at B3LYP/6-31G*, B3LYP/6-31+G**, MPW1PW91/6-31G*, and MPW1PW91/6-31+G** levels of theory. The calculation results suggest a molecular mechanism of a concerted nonsynchronous six-membered cyclic transition state process. The analysis of bond order and natural bond orbital charges implies that the bond polarization of C(=O)O–C, in the sense of C(=O)O^{δ-}...C^{δ+}, is rate determining. The experimental and theoretical parameters have been found to be in reasonable agreement.

1. Introduction

Amino acids of low molecular weight are solids that on heating sinter or decompose into amorphous materials. Moreover, their insolubility in organic solvents and tendency to form zwitterionic species in aqueous solution makes it difficult to study the amino acids decomposition in gas phase as neutral molecules. Despite these limitations, the kinetics of the gas phase elimination of N,N-dimethylglycine,¹ picolinic acid,² and N-phenylglycine,³ and their ethyl ester have been reported. These amino acids as substrate or as intermediate of corresponding ethyl ester decomposed very fast to give CO₂ gas and the corresponding amino compound [reaction 1].^{1–3}



The mechanism of reaction 1 differs from the gas-phase elimination of several types of 2-substituted carboxylic acids which are found to decarboxylate^{4–10} as described in reaction 2.



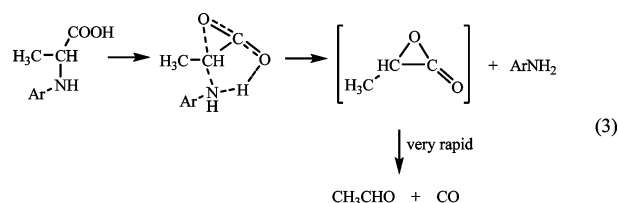
L = leaving group: Cl, Br, OH, OR, OPh, OAc.

* To whom correspondence should be addressed.

[†] Venezolano de Investigaciones Científicas.

[‡] Universidad Central de Venezuela.

However, the gas-phase pyrolysis of 2-(N-Arylamino)propanoic¹¹ was reported to give ArNH₂, CH₃CHO, and CO as final products. The mechanism was thought to involve a five-membered cyclic transition state depicted in reaction 3.



Reaction 3 appears to follow a process similar to reaction 2. The factors affecting the decomposition mechanism of neutral amino acids in the gas phase are thus uncertain. The mechanisms of reactions 1 and 2 create a conflict when comparing PhNHCH₂COOH³ to PhNHCH(CH₃)COOH,¹¹ with the only difference when the H at the α -C is replaced by the CH₃. To have more information about the decomposition process of this type of amino acids, the present work was addressed to study the gas-phase elimination kinetics of PhCH₂NHCH₂COOH, that is, N-benzylglycine and its ethyl ester, to find whether mechanism 1 or mechanism 3 takes place. Moreover, we additionally carried out a theoretical study of the reaction at several computational levels and compare the estimated parameters with the experimental results.

2. Experimental Sections

Ethyl N-Benzylglycidate. This substrate (Aldrich) of 97.0% purity (GC-MS: Saturn 2000 Varian, with a DB-5MS capillary column 30 m × 0.53 mm. I.D., 0.53 μ m film thickness) was used. The quantitative chromatographic analysis of ethylene

product was determined by using a Porapak Q column. The identification of the product N-benzylmethylamine was made with a Varian Saturn 2000 GC-MS instrument with a DB-5MS capillary column.

N-Benzyl Glycine. We wanted to examine the elimination kinetics of N-benzylglycine as a neutral amino acid. For this purpose, N-benzylglycine was prepared from N-benzylglycine hydrochloride (Aldrich) by treatment with 10% NaOH solution. Unfortunately, the prepared amino acid N-benzylglycine, which is a solid, could not be examined in the gas phase due to its insolubility in most inert organic solvents. Solid substrates can not be examined in our static system. N-benzylglycine is very soluble in water, forming a zwitterion specie, which limits its examination as neutral molecules in the gas phase. Our procedure requires that we dissolve the substrate in an inert solvent and then inject the material into the reactor.

Kinetics. The kinetic determinations were performed in a static reaction system as described before.^{12–14} At each temperature, 6–9 runs have been carried out in our experiments. The rate coefficients for the ethyl ester decomposition were calculated from the pressure increase manometrically and/or by formation of ethylene product. The temperature was maintained within ± 0.2 °C through control with a Shinko DC-PS resistance thermometer controller and was measured with a calibrated iron constant thermocouple. No temperature gradient was observed along the reaction vessel. The substrate was dissolved in dioxane and injected directly into the reaction vessel with a syringe through a silicone rubber septum. The amount of substrate used for each reaction was ~ 0.05 to 0.1 mL.

3. Computational Method and Model

The thermal elimination reaction of ethyl N-benzylglycidate was studied using electronic structure methods to gain insight into the kinetics and its mechanisms. The methods used included Møller–Plesset perturbation MP2/6-31G and DFT B3LYP/6-31G, B3LYP/6-31G*, and B3LYP/6-31++G** as implemented in Gaussian 98W.¹⁵ The results indicate that the ethyl ester of N-benzylglycine decomposes to give N-benzylglycine and ethylene in a slow step. The subsequent decarboxylation reaction of unstable intermediate benzylglycine was also studied to determine unequivocally the rate determining step of the reaction. Structures for reactants and products were optimized at each theory level. The transition states were searched and optimized using synchronous transit (QST2, QST3) methodologies. The Berny analytical gradient optimization routines were used. The requested convergence on the density matrix was 10^{-9} atomic units, the threshold value for maximum displacement was 0.0018 Å, and that for the maximum force was 0.00045 hartree/bohr. The nature of the stationary points was established by calculating and diagonalizing the Hessian matrix (force constant matrix). TS structures were characterized by means of normal-mode analysis. The transition vector (TV) associated with the unique imaginary frequency, that is, the eigenvector associated with the unique negative eigenvalue of the force constant matrix has been characterized.

Thermodynamic quantities such as the zero point vibrational energy (ZPVE), the temperature corrections to $E(T)$, and the absolute entropies $S(T)$, were obtained by frequency calculations. The rate coefficient can then be estimated assuming that the transmission coefficient is equal to 1. Temperature corrections and absolute entropies were obtained assuming ideal gas behavior from the harmonic frequencies and moments of inertia by standard methods.¹⁶ Scaling factors for frequencies and zero point energies are taken from the literature.¹⁷

TABLE 1: Temperature and Pressure Data for Pyrolysis Reaction

compound	temperature (°C)	P_0 (torr)	P_f (torr)	P_f/P_0	ave
ethyl ester N-benzylglycine	396.1	34.3	94.3	2.8	2.9
	407.1	26.0	72.0	2.8	
	416.5	22.0	67.0	3.1	
	426.7	25.2	74.3	3.0	

TABLE 2: Stoichiometry of the Elimination Reaction

compound	temperature (°C)	parameter	value				
ethyl ester N-benzylglycine	407.6	time (min)	2.5	5.5	9.5	11.5	16
		reaction (%) (pressure, torr)	23.8	42.2	57.3	68.5	76.8
		ethylene (%) (GC)	21.4	42.2	59.9	71.3	79.6

The first order rate coefficient $k(T)$ was calculated using the TST^{18,19} and assuming that the transmission coefficient is equal to 1, as expressed in the following relation:

$$k(T) = (KT/h) \exp(-\Delta G^\ddagger/RT)$$

where ΔG^\ddagger is the Gibbs free energy change between the reactant and the transition state and K and h are the Boltzmann and Plank constants respectively.

ΔG^\ddagger was calculated using the following relations:

$$\Delta G^\ddagger = \Delta H^\ddagger - T\Delta S^\ddagger$$

and

$$\Delta H^\ddagger = V^\ddagger + \Delta(ZPVE) + \Delta E(T)$$

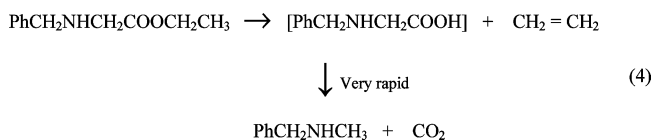
V^\ddagger is the potential energy barrier, and $\Delta(ZPVE)$ and $\Delta E(T)$ are the differences of ZPVE and temperature corrections between the TS and the reactant, respectively.

Frequency calculations were carried out at the same level of theory used for optimization for consistency. Thermodynamic quantities such as zero point vibrational energy (ZPVE), temperature corrections ($E(T)$), energy, and enthalpy energies were obtained from vibrational analysis performed at $T = 400$ C.

4. Results and Discussion

4.1. Experimental Results. N-Benzylglycine was prepared from N-Benzylglycine hydrochloride (Aldrich). Unfortunately, the solid neutral amino acid could not be examined in the gas phase due to its insolubility in most inert organic solvents.

The molecular decomposition of ethyl ester of N-benzylglycine in the gas phase proceeds according to reaction 4:



The stoichiometry of reaction 4 requires that for long reaction time a 3-fold increase in the final pressure, P_f , is required, that is, $P_f = 3P_0$, where P_0 is the initial pressure. The average

TABLE 3: Homogeneity of the Reaction

compound	temperature (°C)	S/V (cm ⁻¹) ^a	10 ⁴ k ₁ (s ⁻¹) ^b	10 ⁴ k ₁ (s ⁻¹) ^c
ethyl ester N-benzylglycine	407.1	1	16.39 ± 0.50	15.61 ± 0.39
		6	15.28 ± 0.45	16.99 ± 0.40

^a S = surface area (cm²); V = volume (cm³). ^b Clean Pyrex vessel. ^c Vessel seasoned with allyl bromide.

TABLE 4: Effect of the Inhibitor Toluene on Rates^a

compound	temperature (°C)	P _s (torr)	P _i (torr)	P _i /P _s	10 ⁴ k ₁ (s ⁻¹)	
ethyl ester N-benzylglycine	407.1	38.0			16.39 ± 0.50	
			33.0	48	1.5	15.60 ± 0.57
			32.5	76	2.3	16.08 ± 0.57
			34.0	105	3.1	16.74 ± 0.40

^a P_s = pressure of the substrate; P_i = pressure of the inhibitor. Vessel seasoned with allyl bromide.

experimental, P_i/P₀ values at four different temperatures and after 10 half-lives is 2.9 (Table 1).

Additional checking of stoichiometry (4) was possible by comparing, up to 75% decomposition, the pressure measurements with the results of quantitative chromatographic analyses of the product ethylene (Table 2).

To examine the effect of the surface on the rate of elimination, several runs in the presence of toluene inhibitor were carried out in a Pyrex vessel with a surface-to-volume ratio of six times greater than the normal vessel, which is equal to one. Studies were carried out in both clean Pyrex vessels and after seasoning the reactors via in situ pyrolysis of allyl bromide. No discernible effects on the reaction were observed (Table 3), which suggests that there is no significant heterogeneous component to the reaction.

The effect of the addition of different proportions of toluene inhibitor is described in Table 4. However, the experiments of the amino ester were always carried out in seasoned vessels and in the presence of at least an equal amount of toluene in order to impede any possible free radical chain reaction. No induction period was observed and the rates were reproducible with a relative standard deviation not greater than 5% at a given temperature.

The first-order rate coefficients of this amino ester, expressed from k₁ = -(2.303/t) log [(3P₀ - P_t)/2P₀] were invariable to initial pressures (Table 5). A plot of log(3P₀ - P_t) against time t gave a good straight line up to 75% reaction (Figure 1). The k-value from Figure 1 is estimated as follows: k₁ = -2.303 × slope (slope = -0.00044 at 396.4 °C) of the straight line at a given temperature. The temperature dependence of the rate coefficients and the corresponding Arrhenius equation is given

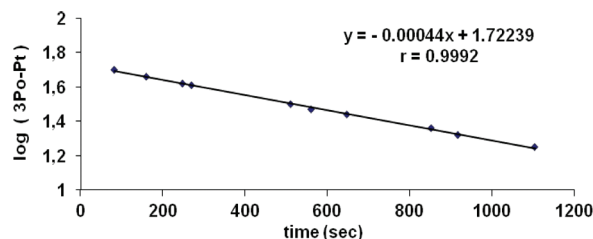


Figure 1. Plot of log(3P₀ - P_t) against time at 396.4 °C.

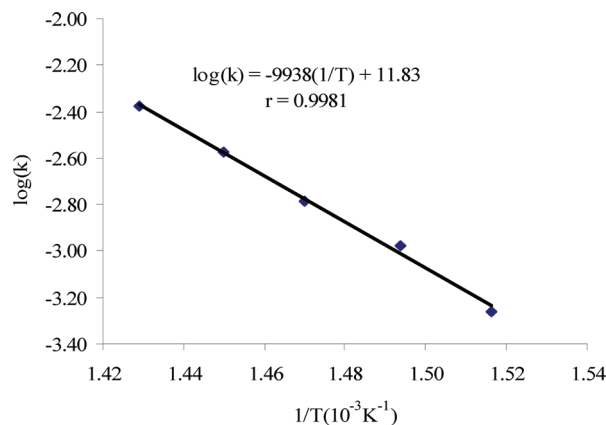
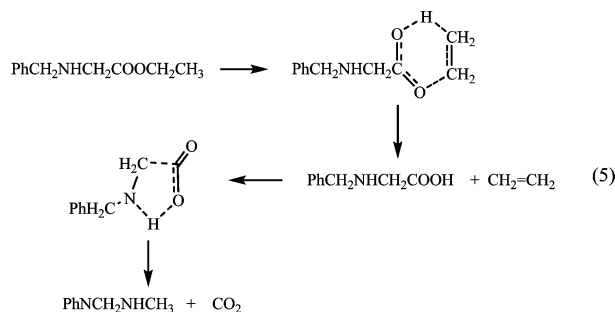


Figure 2. Arrhenius plot for the elimination kinetic of ethyl ester of N-benzylglycine in the gas phase.

in Table 6, Figure 1 (90% confidence coefficient obtained from the least-squares procedure).

According to the results shown in Table 6, the most probable mechanism for the elimination of ethyl ester of N-benzylglycine is described in reaction 5. In this respect, a theoretical study has been carried out to verify or modify the proposed mechanism 5.



4.2. Theoretical Results. 4.2.1. Kinetic and Thermodynamic Parameters. The elimination of ethylene from the N-benzylglycine ethyl ester was studied using various

TABLE 5: Variation of Rate Coefficients with Initial Pressure^{a,b}

substrate	temperature (°C)	parameters				value	
		P ₀ (torr)	10 ⁴ k ₁ (s ⁻¹)	16.7	27.7	32.5	40.0
ethyl ester	407.2						
N-benzylglycine				16.74 ± 0.40	16.39 ± 0.50	16.05 ± 0.46	16.00 ± 0.41

^a Vessel seasoned with allyl bromide. ^b In the presence of the inhibitor toluene.

TABLE 6: Temperature Dependence of the Rate Coefficients^a

substrate	parameters	value				
		temp. (°C)	386.4	396.4	407.1	416.5
ethyl ester						
N-benzylglycine	10 ⁴ k ₁ (s ⁻¹)	5.49 ± 0.01	10.50 ± 0.38	16.39 ± 0.37	26.70 ± 0.09	41.74 ± 0.42

^a Rate equation log k₁ (s⁻¹) = (11.83 ± 0.52) - (190.3 ± 6.9) kJ mol⁻¹ (2.303RT)⁻¹; r = 0.9995.

TABLE 7: Kinetic and Thermodynamic Parameters for the Pyrolysis at 400 °C (673.15 K) of N-Benzylglycine Ethylester

	ΔH^\ddagger (kJ/mol)	ΔG^\ddagger (kJ/mol)	ΔS^\ddagger (J/K mol)	E_a^\ddagger (kJ/mol)	log A
experimental	182.7	207.2	-36.38	188.3	11.68
B3LYP/6-31G*	193.4	189.1	6.39	199.0	13.92
B3LYP/6-31+G**	179.7	178.5	1.78	185.3	15.21
MPW1PW91/6-31G*	201.8	206.4	-6.88	207.4	13.22
MPW1PW91/6-31+G**	187.4	195.2	-11.49	193.0	12.98
PBE/6-31G*	173.3	174.4	-1.51	167.7	13.50
PBE/6-31+G**	154.6	160.3	-8.40	160.2	13.14

electronic structure methods. The derived kinetic and thermodynamic parameters are shown in Table 7. E_a is Arrhenius activation energy, and A is the pre-exponential factor in Arrhenius equation $k = A \exp(-E_a/RT)$. The experimental E_a allows the estimation of ΔH^\ddagger . We compare the experimental values with the parameters from theoretical calculations in Table 7.

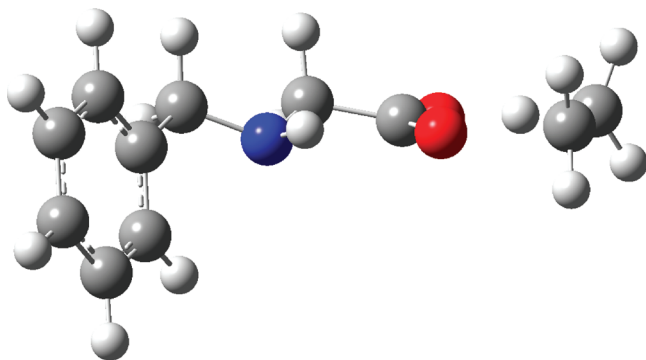
Theoretical parameters E_a^\ddagger and ΔH^\ddagger were found in better agreement with experimental values at DFT method B3LYP/6-31+G**; also MPW1PW91/6-31+G** are in reasonable agreement. Entropy deviations are due to the use of the harmonic approximation and the presence of low-frequency modes, which are highly anharmonic. However, we found that the error in entropy calculations is smaller when using MPW1PW91/6-31+G**. DFT functionals B3LYP and MPW1PW91 performance was better and larger basis set including polarization functions and diffuses improved the results as expected.

The second step, that is, the decarboxylation was also examined and it was found to be faster than the first step of the reaction. The estimated value for decarboxylation is $E_a = 56.30$ kJ/mol at the B3LYP/6-31G** level of theory. Consequently, the rate determining step is the ethylene elimination.

4.2.2. Transition State and Mechanism. The calculated transition state for ethylene elimination is a six-membered cyclic structure as shown in Figure 3. Geometric parameters for reactant and transition state at B3LYP/6-31+G** level are shown in Tables 8 and 9. Atom numbers are illustrated in Scheme 1 for clarity.

Atom distance O22-C23 has increased considerably in the TS compared to reactant, indicating bond breaking. Also the C26-H29 distance is augmented on the TS, while C23-C26 bond is shortening due to the hybridization changing from sp^3 to sp^2 as the double C=C bond forms. Furthermore H29-O21 distance is decreasing as the new O-H bond forms.

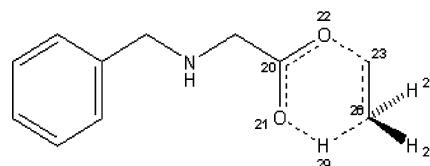
The changes in atom distances suggest that the reaction is dominated by the breaking of O22-C23 bond, which is elongated by 0.57 Å, while the change in C26-H29 bond

**Figure 3.** The TS atoms in ethylene elimination are in the same plane.**TABLE 8: Geometric Parameters**

	interatomic distances (Å)		
	ester	TS	amino acid
C20-O21	1.214	1.277	1.348
C20-O22	1.350	1.269	1.215
O22-C23	1.454	2.028	3.831
C23-C26	1.521	1.405	1.337
C26-H29	1.093	1.312	2.446
H29-O21	2.902	1.321	1.215

TABLE 9: Dihedral Angles in TS Structure

	dihedral angles (°)		
	ester	TS	amino acid
O21-C20-O22-C23	-2.011	12.332	10.243
C20-O22-C23-C26	-86.883	-1.856	-88.895
O22-C23-C26-H29	64.664	-4.289	35.967
C23-C26-H29-O21	-6.591	8.966	175.881
C26-H29-O21-C20	-50.684	0.304	95.854
H29-O21-C20-O22	42.665	-12.605	-1.042

SCHEME 1

distance is smaller (0.22 Å). To better understand the relative progress in the formation and breaking of the bonds involved in the reaction, an analysis of NBO bond orders is presented in the next section. The TS topology is a six-member ring close to planar with small deviations as seen in dihedral angles (Table 9).

4.2.3. Natural Bond Orbital (NBO). NBO calculations were carried to obtain charges and carry out NBO bond order calculations.²⁰⁻²² Wiberg bond indexes²³ were computed using the natural bond orbital NBO program²⁴ as implemented in Gaussian 98W, to further investigate the nature of the TS along the reaction pathway.

Bond breaking and making process involved in the reaction mechanism can be monitored by means of the synchronicity (Sy) concept proposed by Moyano et al.²⁵ defined by the expression:

$$Sy = 1 - \left[\sum_{i=1}^n |\delta B_i - \delta B_{av}| / \delta B_{av} \right] / 2n - 2$$

where n is the number of bonds directly involved in the reaction and the relative variation of the bond index is obtained from:

$$\delta B_i = [B_i^{TS} - B_i^R] / [B_i^P - B_i^R]$$

where the superscripts R, TS, and P, represent reactant, transition state, and product, respectively.

The evolution in bond change is calculated as:

$$\%Ev = \delta B_i \times 100$$

The average value is calculated from:

$$\delta B_{\text{ave}} = 1/n \sum_{i=1}^n \delta B_i$$

In this analysis, the B_i values indicate bond order and δB_i is the change in bond order as the reaction progress from reactant (B_i^R), to the transition state TS (B_i^{TS}) and to products (B_i^P). The percent evolution %Ev is used to show the relative advance of the different reaction coordinates considered. The synchronicity parameter Sy varies between 0 and 1, with a value of Sy = 0 for asynchronous processes and Sy = 1 for a concerted synchronic.

This study was carried out for the rate-determining step. Bonds indexes were calculated for those bonds that change as the reaction proceeds, that is: C20–O21, C20–O22, O22–C23, C23–C26, C26–H29, and O21–H29 (Scheme 1, Figure 2). The remaining bonds stay practically unchanged.

NBO charges also show a strong O22–C23 bond polarization in the sense $O^{\delta-}-C^{\delta+}$. NBO charges and charge density plots of the TS can be found as Supporting Information.

The relative advance in the reaction coordinate (%Ev, Table 10) suggests that the most important factor in the thermal elimination of ethylene is the breaking of bond O22–C23 67%. This fact has also been described in several theoretical works on other related elimination reactions, where the breaking of C–O bond is more advanced than the migration of the hydrogen, demonstrating an asynchronous process.^{26,27} This is also observed in the atom distances in Table 8 as describe above. The migration of hydrogen H29 to oxygen O21 has advanced to a lesser extent than the breaking of O22–C23, as well as the change in bond order in C20–O21 associated with it. In other words, the elongation of the O–C bond of the alcohol part of the ester is dominating in the reaction, and it is accompanied in less extent, by the abstraction of hydrogen at the ethyl group by the carbonyl oxygen. These facts indicates that the breaking of C–O bond occur before the hydrogen transfer indicating a late TS in this reaction coordinate. The described changes in bond order demonstrate asymmetric TS. The synchronicity value of 0.88 reveals a process that is concerted but not completely synchronic.

5. Conclusions

The thermal decomposition of N-benzyl glycine ethyl ester has been studied both experimental and theoretically. The reaction proceeds in two steps, the elimination of ethylene followed by the rapid decarboxylation of the intermediate amino acid N-benzyl glycine to give benzylmethylamine. The formation of benzyl methylamine appears to support mechanism (5). The elimination of the ethyl ester is unimolecular in the presence of the free chain radical suppressor and follows the rate expression $\log k_1 \text{ (s}^{-1}\text{)} = (11.83 \pm 0.52) - (190.3 \pm 6.9) \text{ kJ mol}^{-1} (2.303 \text{ RT})^{-1}$. The study of the potential energy surface at various theory levels showed that the density functional B3LYP with the basis set 6-31+G** was adequate and provided results in accord with the experimental values. The results of the theoretical calculation results appears to support the proposed reaction mechanism in which the substrate N-benzylglycine ethyl ester first decomposes to ethylene in a rate-determining step through a cyclic six-member TS to produce the amino acid N-benzylglycine followed by a rapid decarboxylation to benzyl methylamine. The reaction is governed by the breaking of the O–C_{alkyl} bond, which is more advanced in the TS than

TABLE 10: Wiberg Index Evolution Changes and Synchronicity for Ethylene Elimination from N-Benzylglycine Ethyl Ester

atoms	%Ev	synchronicity
C20–O21	60.407	0.88
C20–O22	46.141	
O22–C23	67.244	
C23–C26	31.269	
C26–H29	50.416	
O21–H29	62.901	

the hydrogen abstraction by the carbonyl oxygen. The TS topology is planar and the process is polar in nature, that is, occurring in a concerted but moderately asynchronous fashion.

Acknowledgment. TC is grateful to the Consejo de Desarrollo Científico y Humanístico (C.D.C.H.) for Grant No. PG-03-00-6499-2006.

Supporting Information Available: This information is available free of charge via the Internet at <http://pubs.acs.org>.

References and Notes

- (1) Ensuncho, A.; Lafont, J.; Rotinov, A.; Domínguez, R. M.; Herize, A.; Quijano, J.; Chuchani, G. *Int. J. Chem. Kinet.* **2001**, *33*, 465–471, and references cited therein.
- (2) Lafont, J.; Ensuncho, A.; Rotinov, A.; Domínguez, R. M.; Herize, A.; Quijano, J.; Chuchani, G. *J. Phys. Org. Chem.* **2003**, *16*, 84–88.
- (3) Domínguez, R. M.; Tosta, M.; Chuchani, G. *J. Phys. Org. Chem.* **2003**, *16*, 869–874.
- (4) Safont, V. S.; Moliner, V.; Andres, J.; Domingo, L. R. *J. Phys. Chem. A.* **1997**, *101*, 1859–1865.
- (5) Domingo, L. R.; Andres, J.; Moliner, V.; Safont, V. S. *J. Am. Chem. Soc.* **1997**, *119*, 6415–6422.
- (6) Domingo, L. R.; Pitcher, M. T.; Andres, J.; Moliner, V.; Safont, V. S.; Chuchani, G. *Chem. Phys. Lett.* **1997**, *274*, 422–428.
- (7) Domingo, L. R.; Pitcher, M. T.; Safont, V. S.; Andres, J.; Chuchani, G. *J. Phys. Chem. A.* **1999**, *103*, 3935–3943.
- (8) Rotinov, A.; Chuchani, G.; Andres, J.; Domingo, L. R.; Safont, V. S. *Chem. Phys.* **1999**, *246*, 1–12.
- (9) Chuchani, G.; Domínguez, R. M.; Rotinov, A.; Martín, I. *J. Phys. Org. Chem.* **1999**, *12*, 612–618.
- (10) Chuchani, G.; Domínguez, R. M.; Herize, A.; Romero, R. *J. Phys. Org. Chem.* **2000**, *13*, 757–764.
- (11) Al-Awadi, S. A.; Abdallah, M. R.; Hasan, M. A.; N. A.; Al-Awadi, N. A. *Tetrahedron* **2004**, *60*, 304–3049.
- (12) Maccoll, A. *J. Chem. Soc.* **1955**, 965–973.
- (13) Swinbourne, E. S. *Aust. J. Chem.* **1958**, *11*, 314–330.
- (14) Domínguez, R. M.; Herize, A.; Rotinov, A.; Alvarez-Aular, A.; Visbal, G.; Chuchani, G. *J. Phys. Org. Chem.* **2004**, *17*, 399–408.
- (15) Frisch, M. J.; Trucks, G. W.; Schlegel, H. B.; Scuseria, G. E.; Robb, M. A.; Cheeseman, J. R.; Zakrzewski, V. G.; Montgomery, J. A., Jr.; Stratmann, R. E.; Burant, J. C.; Dapprich, S.; Millam, J. M.; Daniels, A. D.; Kudin, K. N.; Strain, M. C.; Farkas, O.; Tomasi, J.; Barone, V.; Cossi, M.; Cammi, R.; Mennucci, B.; Pomelli, C.; Adamo, C.; Clifford, S.; Ochterski, J.; Petersson, G. A.; Ayala, P. Y.; Cui, Q.; Morokuma, K.; Malick, D. K.; Rabuck, A. D.; Raghavachari, K.; Foresman, J. B.; Cioslowski, J.; Ortiz, J. V.; Stefanov, B. B.; Liu, G.; Liashenko, A.; Piskorz, P.; Komaromi, I.; Gomperts, R.; Martin, R. L.; Fox, D. J.; Keith, T.; Al-Laham, M. A.; Peng, C. Y.; Nanayakkara, A.; Gonzalez, C.; Challacombe, M.; Gill, P. M. W.; Johnson, B.; Chen, W.; Wong, M. W.; Andres, J. L.; Gonzalez, C.; Head-Gordon, M.; Replogle, E. S.; Pople, J. A. *Gaussian 98, Revision A*; Gaussian, Inc.: Pittsburgh, PA, 1998.
- (16) McQuarrie, D. *Statistical Mechanics*, Harper & Row, New York, 1986.
- (17) (a) Foresman, J. B.; Frish A. *Exploring Chemistry with Electronic Methods*, 2nd Edition; Gaussian, Inc.: Pittsburg, PA, 1996. (b) Scale factors in <http://cccbdb.nist.gov/vibscalejust.asp>. (c) Database of Frequency Scaling Factors for Electronic Structure Methods. http://comp.chem.umn.edu/truhlar/freq_scale.htm.
- (18) Benson, S. W. *The Foundations of Chemical Kinetics*; McGraw-Hill: New York, 1960.
- (19) O'Neal, H. E.; Benson, S. W. *J. Phys. Chem.* **1967**, *71*, 2903–2921. Benson, S. *Thermochemical Kinetics*; John Wiley & Sons: New York, 1968.
- (20) Lendvay, G. *J. Phys. Chem.* **1989**, *93*, 4422–4429.

- (21) Reed, A. E.; Weinstock, R. B.; Weinhold, F. *J. Chem. Phys.* **1985**, *83* (2), 735–746.
- (22) Reed, A. E.; Curtiss, L. A.; Weinhold, F. *Chem. Rev.* **1988**, *88*, 899–926.
- (23) Wiberg, K. B. *Tetrahedron* **1968**, *24*, 1083–1095.
- (24) Gaussian NBO version 3.1.
- (25) Moyano, A.; Periclas, M. A.; Valenti, E. *J. Org. Chem.* **1989**, *54*, 573–582.

- (26) Martins, A. *Chem. Phys. Lett.* **2007**, *439*, 8–13.
- (27) (a) Ruiz, A. J.; Loroño, M.; Córdova, T.; Chuchani, G. *J. Mol. Struct: Theochem* **2006**, *769*, 193–197. (b) Mora, J. R.; Tosta, M.; Dominguez, R. M.; Herize, A.; Barroso, J.; Córdova, T.; Chuchani, G. *J. Phys. Org. Chem.* **2007**, *20* (12), 1021–1031.
- (28) HyperChem 7, Hypercube, Inc.

JP9108943